Title

Chromosomal Aberrations in Canine Gliomas Define Candidate Genes and Common Pathways in Dogs and Humans.

Journal

Journal of neuropathology and experimental neurology, 75(7)

ISSN

0022-3069

Authors

Dickinson, Peter J
York, Dan
Higgins, Robert J
et al.

Publication Date

2016-07-01

DOI

10.1093/jnen/nlw042

Peer reviewed

J Neuropathol Exp Neurol
Vol. 75, No. 7, July 2016, pp. 700–710
doi: 10.1093/jnen/nlw042

ORIGINAL ARTICLE

Chromosomal Aberrations in Canine Gliomas Define Candidate Genes and Common Pathways in Dogs and Humans

Peter J. Dickinson, BVSc, PhD, Dan York, BA, PhD, Robert J. Higgins, BVSc, PhD, Richard A. LeCouteur, BVSc, PhD, Nikhil Joshi, MS, and Danika Bannasch, DVM, PhD

Abstract

Spontaneous gliomas in dogs occur at a frequency similar to that in humans and may provide a translational model for therapeutic development and comparative biological investigations. Copy number alterations in 38 canine gliomas, including diffuse astrocytomas, glioblastomas, oligodendrogliomas, and mixed oligoastrocytomas, were defined using an Illumina 170K single nucleotide polymorphism array. Highly recurrent alterations were seen in up to 85% of some tumor types, most notably involving chromosomes 13, 22, and 38, and gliomas clustered into 2 major groups consisting of high-grade IV astrocytomas, or oligodendrogliomas and other tumors. Tumor types were characterized by specific broad and focal chromosomal events including focal loss of the *INK4A*/*B* locus in glioblastoma and loss of the *RB1* gene and amplification of the *PDGFRA* gene in oligodendrogliomas. Genes associated with the 3 critical pathways in human high-grade gliomas (*TP53*, *RB1*, and *RTK*/*RAS*/*PI3K*) were frequently associated with canine aberrations. Analysis of oligodendrogliomas revealed regions of chromosomal losses syntenic to human 1p involving tumor suppressor genes, such as *CDKN2C*, as well as genes associated with apoptosis, autophagy, and response to chemotherapy and radiation. Analysis of high frequency chromosomal aberrations with respect to human orthologues may provide insight into both novel and common pathways in gliomagenesis and response to therapy.

Key Words: Astrocytoma; Brain tumor; Cancer genomics; Copy number alteration; Dog; Glioma; Oligodendroglioma; Single nucleotide polymorphism (SNP).

INTRODUCTION

Canine gliomas bear striking similarities to their human tumor counterparts at many levels, including imaging, histopathology, and biological behavior (1–3). The occurrence of CNS tumors in aged dogs is similar to that in the adult human population with an incidence of approximately 15–20 per 100 000 (4.5% of necropsy cases) in both species (2, 4–6). Gliomas represent approximately 50% of all primary brain tumors in dogs, and all major glioma types and grades seen in humans are present in dogs; however, specific incidence varies compared to humans. Unlike in humans, grade II/III astrocytomas are more common than glioblastomas and grade I pilocytic astrocytomas are rare in dogs. While astrocytic tumors far outnumber oligodendrogliomas in human patients, oligodendrogliomas are seen at a similar frequency as astrocytomas in dogs. More than 90% of canine oligodendrogliomas are high-grade III/anaplastic compared to less than 50% in humans (6–9). There is a striking breed predilection for glioma in dogs with approximately 50% of gliomas occurring in 4 breeds of brachycephalic dog consisting of Boxers, Boston Terriers, French Bulldogs, and Bulldogs (6, 10). Comparative study of these naturally occurring cancers in dogs may provide a powerful tool for improving the understanding of glioma biology across species (11), as well as a valuable model for therapeutic development.

Comprehensive genomic characterization of human gliomas has resulted in major advances in the understanding of glioma biology and the definition of specific subgroups as well as core pathways (12–15). Approximately 75% of high-grade gliomas show genomic changes in 3 major pathways, that is, TP53, RB1, and RTK-RAS-PI3K, with copy number alterations (CNAs) account for a majority of these changes (12). Somatic CNAs are extremely common in cancer and may be key drivers of cancer biology (16). Distinguishing driver alterations from random CNAs that accumulate during tumorigenesis is a major challenge, although integrative analysis of copy number changes and gene expression as well as assessment of CNAs across different cancer types has helped to define key chromosomal events (14, 16–18). Evolutionarily conserved CNAs have been demonstrated for a variety of tumor types that occur in humans and dogs, suggesting common underlying etiologies (11). Assessment of glioma CNAs across

From the Departments of Surgical and Radiological Sciences (PJD, DY, RAL), Pathology, Microbiology and Immunology (RJH), and Population Health & Reproduction (DB), School of Veterinary Medicine, University of California, Davis, and Bioinformatics Core, UC Davis Genome Center (NJ) University of California, Davis, California.

Send correspondence to: Peter J. Dickinson, BVSc, PhD, School of Veterinary Medicine, UC, Davis, Surgical and Radiological Sciences, 2112 Tupper Hall, 1, Shields Ave., Davis, CA 95616. E-mail: pjdickinson@ucdavis.edu

This study was supported by the Center for Companion Animal Health, UC Davis, The Paul C. and Borghild T. Petersen Foundation and the Maxine Adler Endowment.

Supplementary Data can be found at http://www.jnen.oxfordjournals.org

the 2 species may help provide insight into both driver versus passenger and novel aberrations.

Genomic data for gliomas in dogs are limited; however, preliminary assessment of major candidate genes has shown some similarities to human gliomas. Overexpression of cellular proliferation and apoptosis-associated markers such as *EGFR, PDGFRA, VEGFR1, 2, MET, IGFBP2* (9, 19–21), *ERBB2, pERK, pAKT, BCL2, BCL2L1* (21), and the angiogenic factor *VEGF* (22–24) have been reported. Other overexpressed genes also reported in canine glioma include *TERT, MMP2, 9*, and *IL13RA2* (25–27). Moreover, alterations in key components of the 3 major pathways implicated in human gliomagenesis have been documented based on western blot analysis of canine gliomas (28).

Previous genome wide copy number assessment of gliomas in dogs using comparative genomic hybridization (CGH) profiling at 1-Mb intervals revealed extensive genomic alterations with a high incidence of genomic gains particularly chromosomes CFA (*Canis familiaris*) 13, 34, and 38 (29). Clustering by histological type was not demonstrated; and common deletions involving key glioma-related genes such as *P16/P14ARF, PTEN*, and *NF1* or orthologous deletions to human 1p/19q were not found, although amplification of *MYC* and *EGFR* were reported.

This study expands on this previous study utilizing a dog Illumina 170K single nucleotide polymorphism (SNP) array in an expanded group of dog gliomas paired with normal tissue. The broad findings from the previous CGH array were confirmed but higher resolution allowed for the identification of chromosomal aberrations consistent with involvement of the key pathways described in human gliomas. Comparative cytogenetics also identified candidate genes associated with commonly reported large chromosomal losses involving human chromosomes HSA (*Homo sapiens*) 1p/19q as well as highly recurrent alterations in dog gliomas that warrant further comparative analysis of orthologous human chromosomal regions.

MATERIALS AND METHODS

Samples

Primary tumor tissue was obtained at necropsy or from surgical biopsy of clinical cases presented to the University of California, Davis Veterinary Medical Teaching Hospital. Necropsy samples were collected within 30 minutes of death. All samples were snap-frozen in liquid nitrogen for storage. Samples of adjacent tumor tissue were paraffin-embedded and processed for histological analysis. All tumors were histologically classified by a board-certified pathologist according to the World Health Organization (WHO) classification of human tumors of the central nervous system (30). Samples consisted of 4 astrocytomas (grade II), 1 anaplastic astrocytoma (grade III), 6 glioblastomas (grade IV), 5 oligoastrocytomas (2 grade II, 3 grade III) 3 oligodendrogliomas (grade II), and 19 anaplastic oligodendrogliomas (grade III) (Table 1). Control tissues consisted of either white blood cells collected from ethylenediaminetetraacetate (EDTA) blood sample buffy coats, normal liver, or muscle. The J3TBg canine glioma cell line was cultured as previously described (28). Genomic DNA was extracted from control and tumor tissues, and white blood cells using Qiagen kits (Valencia, California).

SNP Analysis

Genome-wide SNP genotyping was performed on 38 paired samples (tumor and nontumor) as well as the cell line J3TBg using the Illumina CanineHD BeadChip with 173 662 markers. CNAs were called using CNVPartition v 3.2.0 (Illumina) algorithm implemented in Genome studio software.

TABLE 1. Tumor Sample Signalment

Sample ID	Breed	Sex	Age Years	Tumor Type
A1	Boxer	M	8	Astrocytoma II
A2	Labrador	MC	7	Astrocytoma II
A3	Jack Russell Terrier	MC	12	Astrocytoma II
A4	Staffordshire Terrier	MC	8	Astrocytoma II
AA1	Boxer	MC	9	Astrocytoma III
GBM1	Keeshond X	FS	10	Glioblastoma
GBM2	Australian Shepherd	MC	9	Glioblastoma
GBM3	Rhodesian Ridgeback	FS	4	Glioblastoma
GBM4	English Bulldog	M	12	Glioblastoma (SDT-3G)
GBM5	Australian Shepherd	FS	2	Glioblastoma (G06A)
GBM6	Labrador X	MC	2	Glioblastoma
OA1	Labrador	MC	10	Oligoastrocytoma II
OA2	Boxer	MC	9	Oligoastrocytoma II
OA3	Boxer	MC	8	Oligoastrocytoma III
OA4	Pit Bull X	MC	4	Oligoastrocytoma III
OA5	Boxer	FS	10	Oligoastrocytoma III
O1	Labrador	FS	12	Oligodendroglioma II
O2	French Bulldog	MC	10	Oligodendroglioma II
O3	English Bulldog	FS	5	Oligodendroglioma II
AO1	Boston Terrier	M	6	Oligodendroglioma III
AO2	French Bulldog	M	3	Oligodendroglioma III
AO3	Boxer	FS	9	Oligodendroglioma III
AO4	Mastiff X	MC	5	Oligodendroglioma III
AO5	French Bulldog	FS	5	Oligodendroglioma III
AO6	French Bulldog	MC	5	Oligodendroglioma III
AO7	Rottweiler X	MC	10	Oligodendroglioma III
AO8	Boxer	FS	11	Oligodendroglioma III
AO9	Boxer	MC	4	Oligodendroglioma III
AO10	Australian Shepherd	MC	4	Oligodendroglioma III
AO11	Staffordshire Terrier	MC	10	Oligodendroglioma III
AO12	West Highland Terrier	MC	4	Oligodendroglioma III
AO13	Boston Terrier	MC	4	Oligodendroglioma III
AO14	Labrador	MC	8	Oligodendroglioma III
AO15	French Bulldog	MC	7	Oligodendroglioma III
AO16	Labrador	FS	10	Oligodendroglioma III
AO17	Boxer	F	13	Oligodendroglioma III
AO18	Labrador	MC	10	Oligodendroglioma III
AO19	English Bulldog	MC	10	Oligodendroglioma III
J3T	Boston Terrier	M	10	Astrocytoma III (cell line)

F, female; FS, female spayed; M, male; MC, male castrated; SDT-3G and G06A are previously published canine glioma cell lines derived from glioblastoma samples GBM4 and GBM5 (24).

SNPs with a quality score of 0 and intensity only SNPs were removed from subsequent analysis. A minimum probe count of 3 was used and a minimum homozygous region of 1 Mb. GC correction was performed later using Nexus software.

Nexus Copy Number v. 7.5.2 (Biodiscovery, Hawthorne, California) was used to determine structural variation in the paired samples. The SNP-FASST2 segmentation Algorithm was used to estimate the final copy number and allelic event calls. The significance threshold for segmentation was set at 1×10^{-6}, also requiring a minimum of 3 probes per segment and a maximum probe spacing of 1 Mb between adjacent probes before breaking a segment. The log ratio thresholds for single copy gain and single copy loss were set at 0.18 and −0.18, respectively. The log ratio thresholds for 2 or more copy gains and homozygous losses were set at 0.6 and −1.0, respectively. The Homozygous Frequency Threshold was set to 0.95. The Homozygous Value Threshold was set to 0.8. The Heterozygous Imbalance Threshold was set to 0.4. The minimum loss of heterozygosity (LOH) length was set at 1 Mb and minimum SNP probe density at 3. Probes were recentered to the median for all samples. Systematic GC wave correction was applied using a linear correction. Data were aligned to CanFam3.1 (31).

Cluster Analysis

Clustering analysis of aberration profiles was done using an average linkage hierarchical clustering algorithm.

Comparisons

Chromosomal regions reported as being significantly different in terms of frequency of an aberration in group A versus group B met a minimum p value of <0.05 based on a 2-tailed Fisher Exact test as well as a minimum of 25% difference in frequencies between the 2 groups. Analysis of regions with constant frequency, and "combined" analysis was done by merging all contiguous regions that met the p value threshold.

Frequency Significance Testing

Testing was done using 2 algorithms. For the Significance Testing for Aberrant Copy number (STAC) algorithm, areas of the genome with a statistically high frequency of aberration ($p < 0.05$) and an aggregate cut off of 25% were identified using the global frequency statistic approach of the STAC method (32). For the Genomic Identification of Significant Targets in Cancer (GISTIC) algorithm, areas of the genome with a statistically high frequency of aberration (Q-bound value <0.05 and G-score cut-off >1.0) corrected for multiple testing using false discovery rate correction (33) were identified using the GISTIC approach (34). G score is a measure of both frequency of occurrence and the magnitude of the copy number change. Regions were reported as both peak regions and extended regions that defined the widest boundaries repeatedly recalculated by leaving out one of the samples each time.

Candidate Pathway Analysis

Because of the small sample size and the specific algorithms used, the likelihood of not detecting some significant CNAs, particularly those within large aberrations was high. Therefore, we used an additional candidate gene approach to assess chromosomal regions associated with genes commonly reported altered in human gliomas and other cancers (12, 35). Data were analyzed using the Nexus Query tool and reported for candidate genes with combined losses, LOH, or gains consistent with proposed gene function and an aggregate cut off of 15% of total samples.

Whole-Genome Sequencing

Validation of selected tumor CNAs with chromosomal losses was done using single-end sequence reads using an Illumina HiSeq 2000 (Illumina, San Diego, California). The reads were aligned to the canFam3 genome using Burrows–Wheeler aligner and sequencing density (bases per 10 kb) for the defined loci was calculated using R (version 3.2.1).

RESULTS

The most striking overall feature of canine glioma copy number analysis was the consistently high incidence of alterations involving specific chromosomes. Gains involving chromosomes 13 and 38 were seen in up to 68% of gliomas combined and over 85% of oligodendrogliomas for specific loci. Alterations at all loci on chromosomes 13 and 38 were seen in at least 30% of all samples. Similarly, specific gains on chromosomes 7, 20, and 35 were seen in at least 50% of all samples and specific losses on chromosomes 12 and 22 were present in approximately 50% and 60% of samples, respectively (Fig. 1). The majority of CNAs were single copy gains or losses. Thirty-two high copy gains and 12 homozygous copy losses were defined involving 13 and 6 tumors, respectively (Supplementary Data Content 1). Homozygous losses in 10/12 events encompassed well-defined tumor suppressor genes including *CDKN2A*, *CDKN2B* (encoding P16, $P14^{ARF}$, and P15), *MTAP, PTEN, NF1, TUSC1, TUSC2, RASSF1, WWOX*, and *DKK1*. Potential oncogenes within high copy number gain regions included *CDH7, BYSL, CCND3, CDC5L, TPBG, RIMS2, MAFA, SHCBP1, LAMA5, ANKRD17, GLI4, ZFP41, PSCA, MAP3K7, MAPK15, PUF60*, and *NRBP2*.

Clustering Analysis

Hierarchical cluster analysis by aberration profile revealed 2 major clusters. One cluster was composed of only astrocytomas consisting of 5/6 glioblastomas and 2/4 grade II astrocytomas. The second cluster contained all 22 oligodendrogliomas, all 5 oligoastrocytoma samples, 2 grade II astrocytomas, and 1 grade III astrocytoma (Fig. 2). No matched normal sample was available for the J3TBg cell line sample; however, analysis of unpaired data for all samples resulted in a similar dendrogram with the J3TBg cell line clustering with the GBM samples (data not shown).

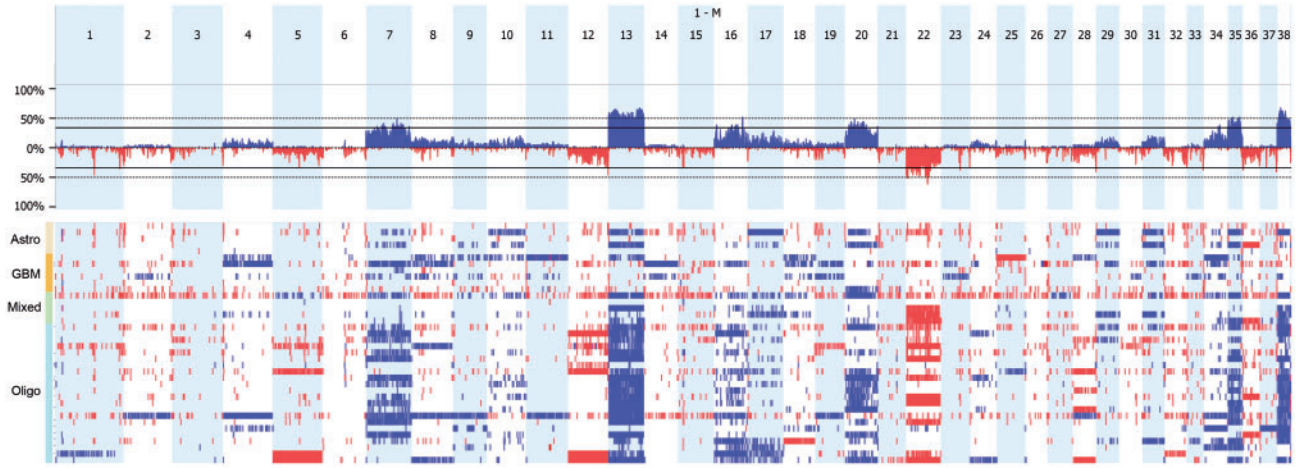

FIGURE 1. Genome plot of copy number events for all samples.

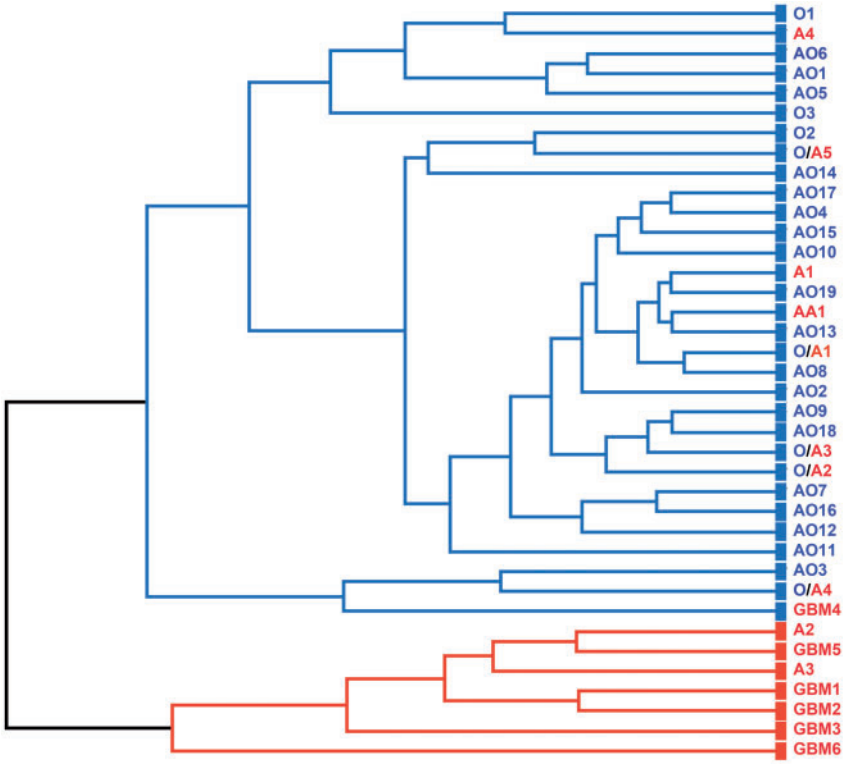

FIGURE 2. Dendrogram for hierarchical clustering of glioma samples showing 2 major clusters. O, oligodendroglioma, AO, anaplastic oligodendroglioma, A, astrocytoma, O/A, oligoastrocytoma, GBM, glioblastoma.

Comparisons

Comparative analysis of aberration profiles was done using the oligodendroglioma and glioblastoma samples. Significant copy number event differences between the 2 tumor types are shown in Fig. 3 (see Supplementary Data Content 2 for details). Significantly different broad events were seen predominantly involving gains on chromosomes 13, 35, and 38 in oligodendrogliomas. Multiple focal aberrations were seen in glioblastomas involving gains on chromosome 14, 18, and 23, and losses on chromosome 25. Additional focal aberrations that were significantly different between tumor types included losses on chromosomes 1, 2, 3, 10, 11, 13, 15, 27, and 33, gains on chromosomes 4, 8, 11, and 19 in glioblastomas, and focal gains on chromosomes 16 and 20 and loss on chromosome 22 in oligodendrogliomas.

Some of the most common differences involved gains on chromosome 13 including amplification of oncogenes *PDGFRA*, *KIT*, *MYC*, and *KDR* that were exclusive to oligodendrogliomas and present in approximately 70% (15/22) of tumors. Focal losses on chromosome 11 involving the *INK4A*

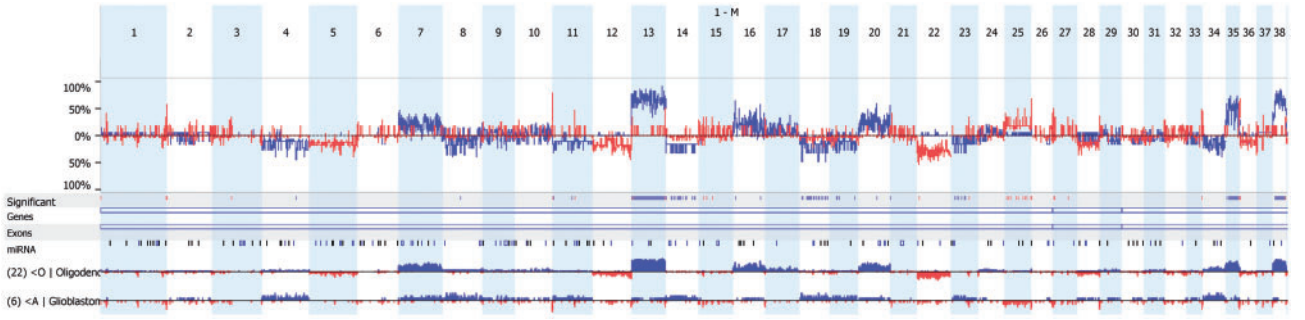

FIGURE 3. Genome plot of copy number events comparing oligodendroglioma and glioblastoma samples. Copy number gains (blue) and losses (red) that are greater in oligodendrogliomas are plotted above the baseline and below the baseline if greater in glioblastomas. Bars in the significance track indicate regions where there is a statistical difference between the 2 groups ($p < 0.05$), and also a minimum threshold difference (25%) in percentage of samples.

locus were present in 50% (3/6) of glioblastomas but only 5% (1/22) of oligodendrogliomas. A focal loss on chromosome 22 including the *RB1* locus was also seen exclusively in approximately 50% (13/22) of oligodendrogliomas. The most frequent aberration seen in glioblastomas involved a focal loss on chromosome 10 in 83% (5/6) of tumors including the *TGFA* locus.

Frequency Analysis

Detailed GISTIC analyses are presented in Supplementary Data Content 3; detailed STAC analyses are presented in Supplementary Data Content 4.

In glioblastomas, GISTIC analysis identified significant aberrations including whole chromosomal gain of chromosome 34 and focal loss of chromosome 11 containing the *INK4A* locus. STAC analysis, which is designed to highlight focal versus broad events, also defined the focal *INK4A* locus loss as significant, in addition to focal losses on chromosomes 2, 3, 10, 13, 15, 17, 21, 23, 26, 28, 33, 35, 36, and 37. Candidate tumor suppressor genes encompassed by these deletions included *CDKN2A, CDKN2B, MTAP, FAS, FOXL2, WDFY1, NCAPG, TRIM40*, and *PAK2*.

In oligodendrogliomas, GISTIC analysis identified significant focal loss on chromosome 15 (containing the *CDKN2C* and *FAF* genes) and focal gains on chromosomes 1 and 20. Significant broad events with G scores >3 were seen involving gains on chromosomes 7, 13, 16, 35, and 38 and losses on chromosomes 5, 12, and 22. More focal aberrations defined in common with both STAC and GISTIC analysis included losses on chromosomes 5 and 15 syntenic to human chromosome 1p, and loss on chromosome 1 syntenic to human chromosome 19q (Fig. 4). Additional aberrations in common included losses on chromosomes 12, 22, 23, 33, 36, and 37, and gains on chromosomes 16, 20, and 34. Candidate oncogenes and tumor suppressor genes associated with more focal gains and losses, respectively, defined by GISTIC and STAC included the oncogenes *AREG, EREG, EPGN, CXCL3, SHC2, DISP1*, and *CHL1* and tumor suppressor genes *TP73, CDKN2C, FAF1, PCDH11X, CDC16, PF4, ZNF382, ZNF829, ZFP82, CUL2*, and *DACH2*. Genes deleted on chromosome 5 (syntenic to HSA1p) associated with apoptosis, autophagy, or response to radiation or chemotherapy included *ATG4C, USP1, GNB1*, and *CDK11A/B* (Fig. 4).

In astrocytomas, GISTIC analysis identified significant focal gains and losses on chromosome 1 that were also defined by STAC. Additional focal regions identified by STAC that were also defined by GISTIC with extended regions included losses on chromosomes 2, 5, 8, 12, 22, 33, and 37. No losses involving the *INK4A* locus were present. Candidate oncogenes and tumor suppressor genes included the oncogenes *CDH7* and tumor suppressor genes *CDC14B, APC, TMEM132A, ANP32A, CDKN2C, FAF1, EPB41L4A, NCAPG, FGFRL1, GAK, LXN, RARRES1, FOXL2, WDFY1*, and *DACH2*.

In oligoastrocytomas, STAC analysis identified significant gains on chromosomes 7 and 13, and losses on chromosomes 26, 36, and X. Candidate oncogenes and tumor suppressor genes included the oncogenes *AREG, EREG, EPGN, CXCL3*, and *PPBP* and tumor suppressor genes *FAS, VBP1*, and *SPRY3*.

RB1 Pathway

Copy number loss/LOH of *RB1* or genes encoding associated proteins P16, P15, and P18 was present in over 70% (27/38) of glioma samples, with *RB1* gene loss present in 27% (3/11) of astrocytomas, 60% (13/22) of oligodendrogliomas, and 80% (4/5) of oligoastrocytomas. Amplification of *CDK4* or *CDK6* genes was present in only one sample (GBM1) (Fig. 5A).

TP53 Pathway

Copy number loss/LOH of *TP53* or genes encoding P14ARF or P21 was present in 37% (14/38) of glioma samples. Amplification of the TP53 inhibitor *MDM2* was not present but *MDM4* was amplified in 42% (16/38) of samples. Loss of the TP53 family member gene *TP73* was exclusive to oligodendrogliomas and was present in 36% (8/22) of this tumor type. Loss of the *INK4A/B* locus encoding the P15, P16, and P14ARF proteins was associated with homozygous loss in 4/5 cases (Fig. 5A).

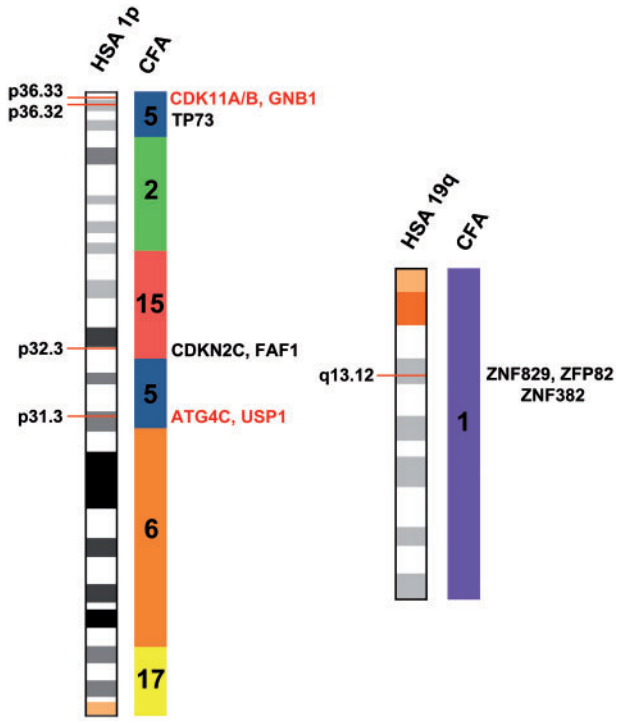

FIGURE 4. Ideogram showing dog chromosomal regions syntenic to human chromosome arms 1p and 19q. Human chromosomes are represented using G banding (centromeric regions in orange) with corresponding syntenic dog regions of chromosomes 2, 5, 6, 15, and 17 represented by colored bars. Deleted regions, identified by STAC and GISTIC algorithms in oligodendroglial tumors are highlighted by red bars showing their corresponding location on the human chromosomes. Candidate tumor suppressor (black) or therapeutic response related genes (red) associated with the deletions are listed to the right of the chromosomes. Deletions for all regions occurred in 36% (8/22) of oligodendrogliomas.

Receptor Tyrosine Kinase Pathways

PDGFRA, *KDR*, and *KIT* were amplified in approximately 50% of gliomas, most consistently associated with large chromosomal gains on CFA13 in oligodendrogliomas. *FGFR1* was amplified in approximately 30% (11/38) of gliomas, predominantly oligodendrogliomas. *EGFR* was amplified in only 1 glioblastoma; however, amplification of EGFR ligands such as *EREG*, *NRG1*, and *EPGN* was present in 35%–50% of glioma samples (Fig. 5B) Alterations in downstream pathways involving PI3K, AKT, and the RAS/RAF/MAPK pathways were common and included amplifications in *PI3K*, *AKT*, and *RAF* (Fig. 5B, C). Copy number losses of the tumor suppressor *PTEN*, including homozygous loss, were seen in approximately 15% (6/38) of gliomas, whereas loss of *NF1* was restricted to a homozygous loss in 1 glioblastoma. Copy number loss or LOH was also seen in the RTK pathway associated tumor suppressors *PHLPP2* and *SPRY2* (Fig. 5C).

Additional Pathways

Additional common alterations involving transcription factors, and the WNT and Hedgehog pathways included amplifications of *MYC*, *ATF6*, *FZD6*, *GLI4*, and *DISP1*, and copy number loss/LOH involving *APC*. Copy number loss or LOH involving the "death receptor" *FAS* was seen in approximately 35% (13/38) of gliomas. Amplification of *EPHA5* was seen in over 60% (24/38) of gliomas (Fig. 5C).

Validation

CNAs were validated in 2 glioblastoma samples (GBM4, 5) using whole-genome sequencing and comparison of sequencing depth with homozygous deletion calls. All homozygous deletions called by Nexus were confirmed by decreased sequence density at the corresponding genomic loci (Fig. 6).

DISCUSSION

Spontaneously occurring gliomas in dogs have long been proposed as a large animal translational model for both delivery strategies and targeted therapies. The latter is in large part dependent on dog tumors having similar molecular genetic abnormalities to those in their human tumor counterparts. Global profiling of human gliomas, mostly glioblastomas, has identified key pathways and lineage-dependent subtypes (eg, proneural, mesenchymal, classical, and neural) (14, 36, 37). The small number of canine glioblastomas analyzed in this study precludes direct comparisons with human subtypes; however, 1 study in humans investigating an unbiased full range of gliomas by gene expression defined essentially the same 2 major glioma groups as in this study, specifically an O group characterized by oligodendroglioma and grade II, III astrocytomas, and a G group predominantly composed of glioblastomas (36). Although specific genes and mechanisms may vary, at a general pathway level, the data presented also suggests that the 3 major pathways implicated in human gliomagenesis are also likely implicated in canine tumors.

Alterations in TP53 pathway signaling in humans may occur through a variety of mechanisms including mutation of *TP53* and altered expression of TP53-related proteins. The current *TP53*-related data demonstrate the potential for alterations of core glioma pathways to occur through different mechanisms across different species. The occurrence of *TP53* gene mutations in dog gliomas is rare (9, 38), although mutations in humans have been reported in approximately 20% of high-grade oligodendrogliomas and 30% of glioblastomas (12, 39, 40). Loss of the *INK4A/B* locus encoding the TP53-related protein $P14^{ARF}$ is also a common finding in human gliomas (12, 40). It was also a defining alteration for dog glioblastomas in this series. By contrast, amplification of the TP53 inhibitor *MDM2*, which is commonly reported in human tumors (12, 41), was not seen in the dog gliomas. Although over 40% of dog gliomas had amplification of *MDM4*, a much less frequently reported alteration in human gliomas. Amplification of *MDM4* has been previously reported in specific populations of anaplastic oligodendrogliomas in humans, associated with amplification of *PIK3C2B* and without *TP53* mutations (42, 43); that was also the case in the dog tumors. This finding may reflect the much higher incidence of anaplastic oligodendrogliomas (>90%) in dogs compared to human

A

	Retinoblastoma Pathway							TP53 Pathway					
	CFA 22 RB1	CFA 11 CDKN2A	CFA 11 CDKN2B	CFA 15 CDKN2C	CFA 10 CDK4	CFA 14 CDK6		CFA 5 TP53	CFA 11 CDKN2A	CFA 12 CDKN1A	CFA 10 MDM2	CFA 38 MDM4	CFA 5 TP73
A1													
A2	LOSS			LOSS									
A3													
A4													
AA1	LOSS			LOSS									
GBM1	LOSS, LOH	LOH	LOH	LOH	LOH	GAIN		LOH	LOH	LOH	LOH	LOSS, LOH	LOH
GBM2		LOSS	LOSS						LOSS				
GBM3													
GBM4		HOM LOSS	HOM LOSS						HOM LOSS				
GBM5		HOM LOSS	HOM LOSS	LOSS					HOM LOSS				
GBM6	LOH			LOSS				LOH		LOH		GAIN	LOH
OA1	LOSS			LOSS								GAIN	
OA2	LOSS											GAIN	
OA3	LOSS											GAIN	
OA4		HOM LOSS	HOM LOSS						HOM LOSS				
OA5	LOSS			LOH						LOH			
O1													
O2		HOM LOSS	HOM LOSS						HOM LOSS				
O3												GAIN	
AO1												GAIN	
AO2												GAIN	
AO3	LOSS							LOSS		LOSS			LOSS
AO4	LOSS											GAIN	
AO5												GAIN	
AO6	LOH											GAIN	
AO7	LOSS	GAIN	GAIN	LOSS, LOH		LOH		LOH	GAIN	LOH		GAIN	LOH
AO8	LOSS			LOSS								GAIN	LOSS
AO9	LOSS, LOH							LOSS, LOH		LOSS, LOH		GAIN	LOSS, LOH
AO10	LOSS			LOSS									GAIN
AO11	LOSS			LOSS				LOSS, LOH		LOSS			
AO12	LOSS			LOSS									LOSS, LOH
AO13	LOSS, LOH			LOSS									
AO14	LOSS							LOSS					LOSS
AO15	LOSS			LOSS									LOSS
AO16										LOSS, LOH		GAIN	LOSS
AO17	LOSS, LOH												LOSS
AO18	LOSS, LOH			LOSS		LOH						GAIN	
AO19												GAIN	

B

	RTK Pathway												
	CFA 13 PDGFRA	CFA 16 FGFR1	CFA 18 EGFR	CFA 13 VEGFR2	CFA 13 KIT	CFA 13 EREG	CFA 16 NRG1	CFA 13 EPGN	CFA 34 PIK3CA	CFA 20 PIK3R2	CFA 38 PIK3C2B	CFA 26 PTEN	CFA 9 NF1
A1	GAIN			GAIN		GAIN		GAIN	GAIN				GAIN
A2											LOSS		
A3													
A4										LOSS			
AA1		LOH		GAIN	GAIN		LOH					LOH	LOH
GBM1	LOH	GAIN, LOH		LOH	LOH	LOSS, LOH	GAIN, LOH	LOSS, LOH	GAIN	GAIN	LOSS, LOH	HOM LOSS	LOH
GBM2													
GBM3													LOH
GBM4			GAIN			GAIN		GAIN	GAIN				HOM LOSS
GBM5						LOSS		LOSS					
GBM6	LOH	LOH		LOH	LOH	LOSS, LOH	LOH	LOSS, LOH			GAIN		
OA1	GAIN	GAIN		GAIN	GAIN	GAIN	GAIN	GAIN		GAIN		HOM LOSS	
OA2											GAIN		
OA3	GAIN			GAIN	GAIN	GAIN		GAIN			GAIN		
OA4													
OA5													
O1												LOH	
O2													LOH
O3									GAIN		GAIN		
AO1	GAIN			GAIN	GAIN	GAIN		GAIN		GAIN	GAIN		
AO2	GAIN			GAIN	GAIN	GAIN	GAIN	GAIN			GAIN		
AO3		GAIN				GAIN	GAIN	GAIN					
AO4	GAIN			GAIN	GAIN	GAIN		GAIN		GAIN	GAIN		
AO5	GAIN			GAIN	GAIN	GAIN		GAIN		GAIN	GAIN		
AO6	GAIN			GAIN	GAIN	GAIN		GAIN		GAIN	GAIN		
AO7	GAIN	GAIN	LOH	GAIN, LOH	GAIN	GAIN	GAIN	GAIN	GAIN	LOH	GAIN	LOH	GAIN
AO8	GAIN, LOH	GAIN		GAIN, LOH	GAIN, LOH	GAIN, LOH	GAIN	GAIN		GAIN, LOH	GAIN	LOSS	
AO9	GAIN	GAIN		GAIN	GAIN	GAIN	GAIN	GAIN		GAIN	GAIN		
AO10	GAIN	GAIN		GAIN	GAIN		GAIN					LOSS	
AO11		GAIN		GAIN			GAIN						
AO12	GAIN			GAIN		GAIN		GAIN				LOSS	
AO13	GAIN	GAIN		GAIN	GAIN	GAIN	GAIN	GAIN					
AO14												LOSS	
AO15	GAIN			GAIN	GAIN	GAIN	GAIN	GAIN					
AO16	GAIN	GAIN		GAIN	GAIN	GAIN	GAIN	GAIN			GAIN		
AO17	GAIN			GAIN	GAIN	GAIN	GAIN	GAIN	GAIN				
AO18	GAIN			GAIN	GAIN	GAIN		GAIN			GAIN		
AO19		GAIN	LOSS				GAIN				GAIN		

FIGURE 5. (A–C) Copy number alterations (CNAs) for selected cancer pathway genes are shown for all samples. Copy number gains are shown in blue and losses or loss of heterozygosity (LOH) in red. A, astrocytoma, GBM, glioblastoma, OA, oligoastrocytoma, O, oligodendroglioma, AO, anaplastic oligodendroglioma, CFA, *Canis familiaris*.

C

	RTK Pathway							Other Pathways					
	chr8 AKT1	chr7 AKT3	chr5 PHLPP2	chr20 RAF1	chr22 SPRY2	chr13 MYC	chr38 ATF6	chr13 FZD6	chr3 APC	chr13 GLI4	chr38 DISP1	chr26 FAS	chr13 EPHA5
A1		GAIN		GAIN		GAIN		GAIN		GAIN	GAIN		GAIN
A2									LOSS	LOSS			
A3	LOSS								LOSS	LOSS	CN LOSS		
A4													
AA1		GAIN		GAIN			GAIN	GAIN	LOSS			LOH	GAIN
GBM1	GAIN	GAIN	LOH	LOH	LOH	LOH	LOH	LOH		LOH	CN LOSS	HOM LOSS	LOSS, LOH
GBM2													
GBM3	LOSS									LOSS		LOSS	
GBM4	GAIN							GAIN		GAIN			GAIN
GBM5												LOSS	LOH
GBM6			LOH		LOH	LOH		LOH		LOH			
OA1	LOSS			GAIN		GAIN	GAIN	GAIN	LOSS			LOSS	GAIN
OA2					LOSS								GAIN
OA3					LOSS	GAIN	GAIN	GAIN		GAIN	GAIN		GAIN
OA4													
OA5	GAIN				LOSS		GAIN			GAIN	GAIN	LOSS	
O1						GAIN		GAIN		GAIN			GAIN
O2	LOH												
O3							GAIN		LOH	GAIN	GAIN		
AO1		GAIN		GAIN		GAIN	GAIN	GAIN		GAIN	GAIN		HI COPY GAIN
AO2				GAIN		GAIN	GAIN	GAIN		GAIN	GAIN		GAIN
AO3			LOSS	GAIN				GAIN					GAIN
AO4	LOSS	GAIN		GAIN		GAIN	GAIN	GAIN		GAIN		LOSS	GAIN
AO5				GAIN		GAIN	GAIN	GAIN		GAIN			GAIN
AO6		GAIN		GAIN	LOH	GAIN	GAIN	GAIN		GAIN	GAIN		GAIN
AO7	GAIN, LOH	GAIN	LOH		LOH	GAIN	GAIN	GAIN		GAIN	GAIN	LOH	GAIN
AO8	LOSS			GAIN, LOH		GAIN, LOH	GAIN	GAIN, LOH	LOSS	LOH	GAIN		GAIN, LOH
AO9	GAIN		LOSS,LOH	GAIN	LOSS, LOH	GAIN	GAIN	GAIN		HI COPY GAIN	GAIN		GAIN
AO10	GAIN	GAIN								GAIN	GAIN	LOH	
AO11			LOSS,LOH			GAIN		GAIN	LOSS	GAIN		LOSS	GAIN
AO12		GAIN								GAIN			
AO13				GAIN	LOSS, LOH	GAIN		GAIN	LOSS	GAIN		LOSS	GAIN
AO14					LOSS	GAIN	GAIN	GAIN		GAIN	GAIN		GAIN
AO15	GAIN	GAIN			LOSS		GAIN	GAIN		GAIN		LOSS	GAIN
AO16	LOSS	GAIN				GAIN	GAIN	GAIN					GAIN
AO17		GAIN			LOSS, LOH		GAIN	GAIN		GAIN			GAIN
AO18		GAIN			LOSS, LOH	GAIN	GAIN	GAIN		GAIN	GAIN		GAIN
AO19						GAIN	GAIN				GAIN	LOSS	GAIN

FIGURE 5. Continued

tumors and specifically the predominance of anaplastic oligodendrogliomas in this sample set.

Simultaneous disruption of RB1 and TP53 pathways by a variety of mechanisms is seen in approximately 50% of human anaplastic oligodendrogliomas (41) and over 70% of glioblastomas (12, 13). CNAs involving RB1 and TP53 pathways were seen in 79% and 76% of canine gliomas, respectively; combined with previous protein expression data (28), this supports involvement of these key pathways in a large proportion of canine gliomas. The major differences compared to human RB1 pathway copy number data appear to be a higher incidence of *RB1* and *CDKN2C(P18)* copy number loss (44, 45), fewer losses involving *CDKN2A/B* (P16, P15) (12, 41), and a low incidence of *CDK4* and *CDK6* amplification in canine tumors with only 1 *CDK6* gain in a glioblastoma sample.

As with TP53 and RB1 pathways the RTK-RAS-PI3K key pathways were frequently associated with CNAs, and species differences in specific genes affected were also present. Of note were the high frequency gains associated with *PDGFRA, VEGFRA, FGFR1, KIT, AKT3*, *RAF1*, and *MYC* in 50%–80% of anaplastic oligodendrogliomas. *PDGFRA* amplification is reported variably in different glioma types and grades in humans, but has been specifically associated with the proneural classification that usually encompasses the oligodendrocytic phenotype (14, 37, 46, 47). Overexpression of PDGFRA mRNA and protein has been shown previously for canine high-grade gliomas, further emphasizing the potential role of PDGFRA in gliomagenesis in dogs (19, 20). Although EGFR overexpression has been reported in canine oligodendrogliomas and astrocytomas (9, 19–22), gene amplification commonly seen in human astrocytomas (12), and to a lesser degree in oligodendrogliomas (48, 49), does not appear to be the most likely mechanism for altered expression in dogs based on the current data.

Given the similarity of CNAs across cancer types (16), it is unsurprising that similarities exist across species within the same tumor types. The current and previously published canine data caution that major mechanistic and gene-specific species differences such as lower levels of *EGFR, MDM2* amplification, *NF1* deletion, or *IDH1* gene mutation exist (50). The current data do, however, support the involvement of similar core pathways in human and canine gliomas and the use of canine tumors in translational pathway-targeted studies. Integrated analysis of larger data sets, including mutational, epigenetic, and expression analyses (13, 14, 18, 51), are needed to define the biological significance of common CNAs, the occurrence of specific molecular subtypes relevant to human gliomas, and the validity of more focused pathway targets that may vary between the 2 species.

Beyond validation of canine gliomas as a translational model, cross-species analysis of genomic alterations in similar tumor types my provide insight into both common and novel mechanisms of gliomagenesis and responses to therapy. It is well established that genomic alterations in specific tumors may be evolutionarily conserved across species (11, 52, 53), and the karyotypic differences between the 2 species (dogs have 38 vs 22 autosomes in humans, with the largest chromosome CFA1 being smaller than HSA 12) may allow for more focused analysis of orthologous regions of chromosomal alterations within large human candidate regions. See Supplementary Data Content 5 for comparisons.

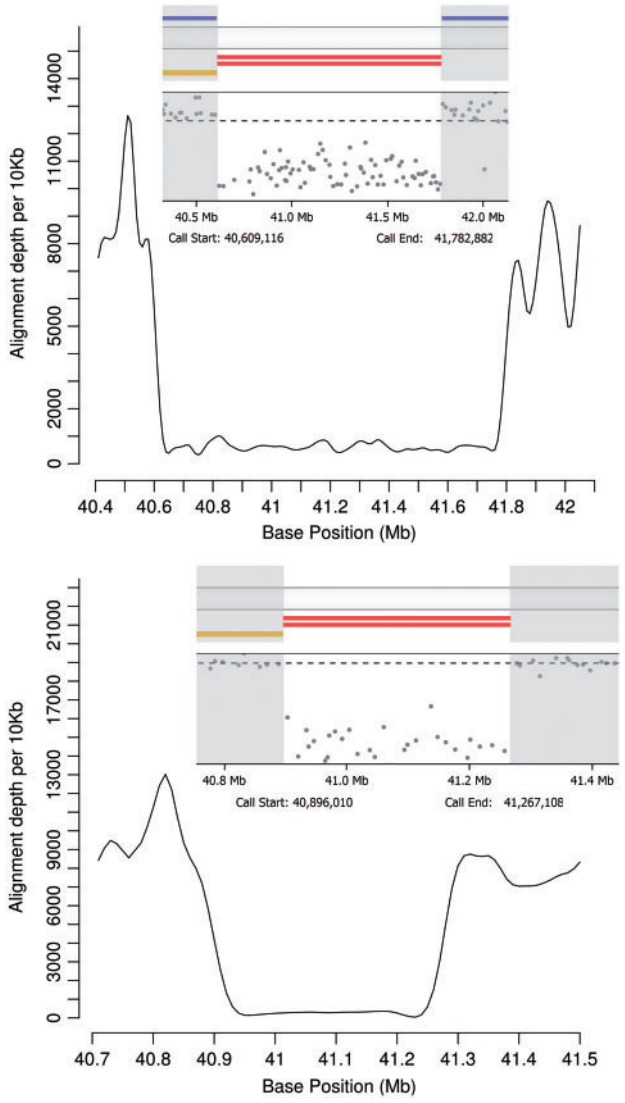

FIGURE 6. Specific CNAs in selected tumors were validated by whole-genome sequencing. Sequencing depth plots for CFA 11 homozygous deletions encompassing the INK4A/B locus are shown for GBM4 (top panel) and GBM5 (bottom panel). Nexus graphical representations of SNP density plots and homozygous deletion calls (double red bars) with corresponding deletion start and end points are shown as inserts.

The most commonly reported CNAs in human glioblastomas involve chromosome 7 gain (with or without *EGFR* amplification), loss of 9p (with or without *CDKN2A* loss), and loss of chromosome 10 (often with *PTEN* loss) (54–59). The current data largely support previous findings for broad events in canine gliomas (29), including amplifications syntenic to *HSA7* (CFA16), although not associated with *EGFR* amplification as previously reported. Additionally, the higher resolution analysis identified *CDKN2A* (HSA 9, CFA11), *PTEN* (HSA 10, CFA 26), and 1p/19q syntenic losses (CFA 5, 15, 1). Given the very high frequency of genomic alterations seen in specific chromosomes in these highly inbred animals, for example, broad gains on CFA 13, 35, and 38 in oligodendrogliomas and CFA 14, 18, and 23 in glioblastoma, it is reasonable to speculate that further comparison to syntenic human regions may reveal key glioma-related genes within these regions (eg, CFA13: HSA 4pq, 8q, 15q; CFA 35: HSA6q; CFA38: HSA1q).

The most commonly reported alteration in human oligodendroglioma involves loss of 1p and 19q either alone or combined (60), although other commonly reported losses include gains on chromosomes 4, 7, 8q, 12, and 16 (42, 54, 60–69). Codeletions involving 1p19q have been consistently associated with a better response to chemotherapy and radiation therapy in humans, with increased progression free and overall survival (70–72). Polysomy of human 1q and 19p has conversely been associated with a poorer prognosis (73). Additionally, 1p19q deletion has been associated anatomically with tumors arising in the frontal lobes or bilaterally but not with tumors arising from the temporal/insular lobes or diencephalon (62, 74). Due to the larger number of small acrocentric chromosomes in dogs, HSA 1p is represented on canine chromosomes 2, 5, 6, 15, and 17 (Fig. 4). Although detailed therapeutic and prognostic data are not available for oligodendrogliomas in dogs, orthologous losses may be informative with respect to biologically significant genes within large human 1p deletions. Contrary to earlier studies, approximately 60% of canine oligodendrogliomas (14/22) had losses syntenic to regions of HSA 1p involving focal losses on chromosomes CFA 5 and CFA 15. These regions encompass candidate tumor suppressor genes potentially associated with gliomagenesis and previously reported in human tumors including FAS-associated factor (*FAF*), *TP73*, and *CDKN2C* (75, 76), as well as several genes specifically on CFA 5 (*CDK11B, GNB1, ATG4C*, and *USP1*), with potential roles in improved response to therapy. Knockdown of the cell cycle protein CDK11B has been shown to increase sensitivity to doxorubicin in liposarcoma and osteosarcoma (77), and the guanidine nucleotide binding protein GNB1 may be an important component of the antiapoptosis pathway (78). ATG4 is required for the autophagic response, which is frequently activated in tumor cells treated with chemotherapy or radiation and may have both anti- and protumor functions. Autophagy has been shown to contribute to resistance of glioma cells to antiangiogenic agents, and inhibition of autophagy sensitizes carcinoma cells to radiation therapy (79, 80). Ubiquitination of proteins such as PCNA and FANCD2 is critical for the DNA damage response and is reversed by hydrolases such as USP1. Downregulation of USP1 has recently been shown to increase apoptosis in temozolamide-treated glioma cells and suppression of USP1 has been suggested as a means to enhance the cytotoxic potential of temozolamide (81).

Eight oligodendrogliomas with deletions syntenic to HSA 1p also had concurrent CFA 1 losses involving regions syntenic to HSA 19q. The deleted region involved a KRAB zinc finger protein cluster including *ZNF420, ZNF382, ZNF829*, and *ZFP82*. Zinc finger proteins are some of the most abundant proteins in the eukaryotic genome and often act as DNA binding transcription factors. Epigenetic silencing of *ZNF342*, also on HSA19q has been implicated in oligodendrogliomagenesis, and *ZNF382 (KS1)* and *ZFP82 (ZNF545)* are both proapoptotic tumor suppressor genes that repress

multiple oncogenes. *ZNF829* is hypermethylated and downregulated in colorectal cancers (82) and ZNF420 (APAK) is known to have important regulatory effects over TP53-mediated apoptosis (83, 84).

In conclusion, high-resolution copy number analysis of canine gliomas suggests that key pathways in human glioma are represented in their dog counterparts although specific affected genes may vary. Comparative analysis of genomically unstable canine chromosomal regions syntenic to HSA 1p/19q in oligodendrogliomas demonstrates the potential to define candidate tumor suppressor genes and genes that may be relevant to therapeutic response in human tumors. Expanded comparative analysis of orthologous alterations across the dog glioma genome is ongoing to define further the key genes in gliomagenesis.

REFERENCES

1. Dickinson PJ. Advances in diagnostic and treatment modalities for intracranial tumors. J Vet Intern Med 2014;28:1165–85
2. Candolfi M, Curtin JF, Nichols WS, et al. Intracranial glioblastoma models in preclinical neuro-oncology: Neuropathological characterization and tumor progression. J Neurooncol 2007;85:133–48
3. Koestner A, Bilzer T, Fatzer R, et al. Histological Classification of Tumors of the Nervous System of Domestic Animals. 2nd ed. Washington, DC: The Armed Forces Institute of Pathology 1999
4. Dolecek TA, Propp JM, Stroup NE, et al. CBTRUS statistical report: Primary brain and central nervous system tumors diagnosed in the United States in 2005-2009. Neuro Oncol 2012;14(Suppl 5):v1–49
5. Dorn CR, Taylor DO, Frye FL, et al. Survey of animal neoplasms in Alameda and Contra Costa Counties, California. I. Methodology and description of cases. J Natl Cancer Inst 1968;40:295–305
6. Song RB, Vite CH, Bradley CW, et al. Postmortem evaluation of 435 cases of intracranial neoplasia in dogs and relationship of neoplasm with breed, age, and body weight. J Vet Intern Med 2013;27:1143–52
7. Ostrom QT, Gittleman H, Fulop J, et al. CBTRUS statistical report: Primary brain and central nervous system tumors diagnosed in the United States in 2008-2012. Neuro Oncol 2015;17(Suppl 4):iv1–iv62
8. Snyder JM, Shofer FS, Van Winkle TJ, et al. Canine intracranial primary neoplasia: 173 cases (1986-2003). J Vet Intern Med 2006;20:669–75
9. Stoica G, Kim HT, Hall DG, et al. Morphology, immunohistochemistry, and genetic alterations in dog astrocytomas. Vet Pathol 2004;41:10–9
10. Truve K, Dickinson P, Xiong A, et al. Utilizing the dog genome in the search for novel candidate genes involved in glioma development—Genome wide association mapping followed by targeted massive parallel sequencing identifies a strongly associated locus. PLoS Genet 2016;12(5):e1006000
11. Schiffman JD, Breen M. Comparative oncology: What dogs and other species can teach us about humans with cancer. Philos Trans R Soc Lond B Biol Sci 2015;370 (1673)
12. Cancer Genome Atlas Research N. Comprehensive genomic characterization defines human glioblastoma genes and core pathways. Nature 2008;455:1061–8
13. Riddick G, Fine HA. Integration and analysis of genome-scale data from gliomas. Nat Rev Neurol 2011;7:439–50
14. Verhaak RG, Hoadley KA, Purdom E, et al. Integrated genomic analysis identifies clinically relevant subtypes of glioblastoma characterized by abnormalities in PDGFRA, IDH1, EGFR, and NF1. Cancer Cell 2010;17:98–110
15. Parsons DW, Jones S, Zhang X, et al. An integrated genomic analysis of human glioblastoma multiforme. Science 2008;321:1807–12
16. Beroukhim R, Mermel CH, Porter D, et al. The landscape of somatic copy-number alteration across human cancers. Nature 2010;463:899–905
17. de Tayrac M, Etcheverry A, Aubry M, et al. Integrative genome-wide analysis reveals a robust genomic glioblastoma signature associated with copy number driving changes in gene expression. Genes Chromosomes Cancer 2009;48:55–68
18. Kotliarov Y, Kotliarova S, Charong N, et al. Correlation analysis between single-nucleotide polymorphism and expression arrays in gliomas identifies potentially relevant target genes. Cancer Res 2009;69:1596–603
19. Dickinson PJ, Roberts BN, Higgins RJ, et al. Expression of receptor tyrosine kinases VEGFR-1 (FLT-1), VEGFR-2 (KDR), EGFR-1, PDGFRalpha and c-Met in canine primary brain tumours. Vet Comp Oncol 2006;4:132–40
20. Higgins RJ, Dickinson PJ, Lecouteur RA, et al. Spontaneous canine gliomas: Overexpression of EGFR, PDGFRalpha and IGFBP2 demonstrated by tissue microarray immunophenotyping. J Neurooncol 2009;98:49–55
21. Ide T, Uchida K, Kikuta F, et al. Immunohistochemical characterization of canine neuroepithelial tumors. Vet Pathol 2010;47:741–50
22. Lipsitz D, Higgins RJ, Kortz GD, et al. Glioblastoma multiforme: Clinical findings, magnetic resonance imaging, and pathology in five dogs. Vet Pathol 2003;40:659–69
23. Dickinson PJ, Sturges BK, Higgins RJ, et al. Vascular endothelial growth factor mRNA expression and peritumoral edema in canine primary central nervous system tumors. Vet Pathol 2008;45:131–9
24. Rossmeisl JH, Duncan RB, Huckle WR, et al. Expression of vascular endothelial growth factor in tumors and plasma from dogs with primary intracranial neoplasms. Am J Vet Res 2007;68:1239–45
25. Long S, Argyle DJ, Nixon C, et al. Telomerase reverse transcriptase (TERT) expression and proliferation in canine brain tumours. Neuropathol Appl Neurobiol 2006;32:662–73
26. Mariani CL, Boozer LB, Braxton AM, et al. Evaluation of matrix metalloproteinase-2 and -9 in the cerebrospinal fluid of dogs with intracranial tumors. Am J Vet Res 2013;74:122–9
27. Debinski W, Dickinson P, Rossmeisl JH, et al. New agents for targeting of il-13ra2 expressed in primary human and canine brain tumors. PLoS One 2013;8:e77719
28. Boudreau CE, York D, Higgins RJ, et al. Molecular signalling pathways in canine gliomas. Vet Comp Oncol 2015; doi:10.1111/vco.12147 [published on line ahead of print March 25, 2015]
29. Thomas R, Duke SE, Wang HJ, et al. 'Putting our heads together': Insights into genomic conservation between human and canine intracranial tumors. J Neurooncol 2009;94:333–49
30. Louis DN, Ohgaki H, Wiestler OD, et al. The 2007 WHO classification of tumours of the central nervous system. Acta Neuropathol 2007;114:97–109
31. Hoeppner MP, Lundquist A, Pirun M, et al. An improved canine genome and a comprehensive catalogue of coding genes and non-coding transcripts. PLoS One 2014;9:e91172
32. Diskin SJ, Eck T, Greshock J, et al. STAC: A method for testing the significance of DNA copy number aberrations across multiple array-CGH experiments. Genome Res 2006;16:1149–58
33. Benjamini Y, Hochberg Y. Controlling the false discovery rate: A practical and powerful approach to multiple testing. J Royal Stat Soc B 1995;57:289–300
34. Beroukhim R, Getz G, Nghiemphu L, et al. Assessing the significance of chromosomal aberrations in cancer: Methodology and application to glioma. Proc Natl Acad Sci U S A 2007;104:20007–12
35. Vogelstein B, Papadopoulos N, Velculescu VE, et al. Cancer genome landscapes. Science 2013;339:1546–58
36. Li A, Walling J, Ahn S, et al. Unsupervised analysis of transcriptomic profiles reveals six glioma subtypes. Cancer Res 2009;69:2091–9
37. Phillips HS, Kharbanda S, Chen R, et al. Molecular subclasses of high-grade glioma predict prognosis, delineate a pattern of disease progression, and resemble stages in neurogenesis. Cancer Cell 2006;9:157–73
38. York D, Higgins RJ, LeCouteur RA, et al. TP53 mutations in canine brain tumors. Vet Pathol 2012;49:796–801
39. Hagel C, Laking G, Laas R, et al. Demonstration of p53 protein and TP53 gene mutations in oligodendrogliomas. Eur J Cancer 1996;32A:2242–8
40. Hoang-Xuan K, He J, Huguet S, et al. Molecular heterogeneity of oligodendrogliomas suggests alternative pathways in tumor progression. Neurology 2001;57:1278–81
41. Watanabe T, Yokoo H, Yokoo M, et al. Concurrent inactivation of RB1 and TP53 pathways in anaplastic oligodendrogliomas. J Neuropathol Exp Neurol 2001;60:1181–9
42. Talagas M, Marcorelles P, Uguen A, et al. Identification of a novel population in high-grade oligodendroglial tumors not deleted on 1p/19q using array CGH. J Neurooncol 2012;109:405–13

43. Riemenschneider MJ, Buschges R, Wolter M, et al. Amplification and overexpression of the *MDM4 (MDMX)* gene from 1q32 in a subset of malignant gliomas without TP53 mutation or MDM2 amplification. Cancer Res 1999;59:6091–6
44. He J, Hoang-Xuan K, Marie Y, et al. P18 tumor suppressor gene and progression of oligodendrogliomas to anaplasia. Neurology 2000;55: 867–9
45. Pohl U, Cairncross JG, Louis DN. Homozygous deletions of the *CDKN2C*/*p18INK4C* gene on the short arm of chromosome 1 in anaplastic oligodendrogliomas. Brain Pathol 1999;9:639–43
46. Alentorn A, Marie Y, Carpentier C, et al. Prevalence, clinicopathological value, and co-occurrence of PDGFRA abnormalities in diffuse gliomas. Neuro Oncol 2012;14:1393–403
47. Smith JS, Wang XY, Qian J, et al. Amplification of the platelet-derived growth factor receptor-A (*PDGFRA*) gene occurs in oligodendrogliomas with grade IV anaplastic features. J Neuropathol Exp Neurol 2000;59: 495–503
48. Reifenberger J, Reifenberger G, Ichimura K, et al. Epidermal growth factor receptor expression in oligodendroglial tumors. Am J Pathol 1996; 149:29–35
49. Gorlia T, Delattre JY, Brandes AA, et al. New clinical, pathological and molecular prognostic models and calculators in patients with locally diagnosed anaplastic oligodendroglioma or oligoastrocytoma. A prognostic factor analysis of European organisation for research and treatment of cancer brain tumour group study 26951. Eur J Cancer 2013;49: 3477–85
50. Reitman ZJ, Olby NJ, Mariani CL, et al. IDH1 and IDH2 hotspot mutations are not found in canine glioma. Int J Cancer 2010;127:245–6
51. Lo KC, Rossi MR, LaDuca J, et al. Candidate glioblastoma development gene identification using concordance between copy number abnormalities and gene expression level changes. Genes Chromosomes Cancer 2007;46:875–94
52. Breen M, Modiano JF. Evolutionarily conserved cytogenetic changes in hematological malignancies of dogs and humans–man and his best friend share more than companionship. Chromosome Res 2008;16:145–54
53. Roode SC, Rotroff D, Avery AC, et al. Genome-wide assessment of recurrent genomic imbalances in canine leukemia identifies evolutionarily conserved regions for subtype differentiation. Chromosome Res 2015; 23:681–708
54. Idbaih A, Marie Y, Lucchesi C, et al. BAC array CGH distinguishes mutually exclusive alterations that define clinicogenetic subtypes of gliomas. Int J Cancer 2008;122:1778–86
55. Korshunov A, Sycheva R, Golanov A. Genetically distinct and clinically relevant subtypes of glioblastoma defined by array-based comparative genomic hybridization (array-CGH). Acta Neuropathol 2006;111: 465–74
56. Maher EA, Brennan C, Wen PY, et al. Marked genomic differences characterize primary and secondary glioblastoma subtypes and identify two distinct molecular and clinical secondary glioblastoma entities. Cancer Res 2006;66:11502–13
57. Misra A, Pellarin M, Nigro J, et al. Array comparative genomic hybridization identifies genetic subgroups in grade 4 human astrocytoma. Clin Cancer Res 2005;11:2907–18
58. Nigro JM, Misra A, Zhang L, et al. Integrated array-comparative genomic hybridization and expression array profiles identify clinically relevant molecular subtypes of glioblastoma. Cancer Res 2005;65:1678–86
59. Crespo I, Tao H, Nieto AB, et al. Amplified and homozygously deleted genes in glioblastoma: Impact on gene expression levels. PLoS One 2012;7:e46088
60. Reifenberger J, Reifenberger G, Liu L, et al. Molecular genetic analysis of oligodendroglial tumors shows preferential allelic deletions on 19q and 1p. Am J Pathol 1994;145:1175–90
61. Jeuken JWM, Boots-Sprenger SHE, Wesseling P. Chromosomal imbalances in oligodendroglial tumors as detected by comparative genomic hybridization (CGH). In: Zhang W, Fuller GN, eds. *Genomic and Molecular Neuro-Oncology*. Sudbury, MA: Jones and Bartlett 2004: 185–98
62. Kouwenhoven MC, Gorlia T, Kros JM, et al. Molecular analysis of anaplastic oligodendroglial tumors in a prospective randomized study: A report from EORTC study 26951. Neuro Oncol 2009;11:737–46
63. Jeuken JW, Sprenger SH, Wesseling P, et al. Identification of subgroups of high-grade oligodendroglial tumors by comparative genomic hybridization. J Neuropathol Exp Neurol 1999;58:606–12
64. von Deimling A, Fimmers R, Schmidt MC, et al. Comprehensive allelotype and genetic anaysis of 466 human nervous system tumors. J Neuropathol Exp Neurol 2000;59:544–58
65. Kotliarov Y, Steed ME, Christopher N, et al. High-resolution global genomic survey of 178 gliomas reveals novel regions of copy number alteration and allelic imbalances. Cancer Res 2006;66:9428–36
66. Zhu JJ, Santarius T, Wu X, et al. Screening for loss of heterozygosity and microsatellite instability in oligodendrogliomas. Genes Chromosomes Cancer 1998;21:207–16
67. Harada S, Henderson LB, Eshleman JR, et al. Genomic changes in gliomas detected using single nucleotide polymorphism array in formalin-fixed, paraffin-embedded tissue: Superior results compared with microsatellite analysis. J Mol Diagn 2011;13:541–8
68. Weber RG, Sabel M, Reifenberger J, et al. Characterization of genomic alterations associated with glioma progression by comparative genomic hybridization. Oncogene 1996;13:983–94
69. Blesa D, Mollejo M, Ruano Y, et al. Novel genomic alterations and mechanisms associated with tumor progression in oligodendroglioma and mixed oligoastrocytoma. J Neuropathol Exp Neurol 2009;68:274–85
70. Cairncross G, Wang M, Shaw E, et al. Phase III trial of chemoradiotherapy for anaplastic oligodendroglioma: Long-term results of RTOG 9402. J Clin Oncol 2013;31:337–43
71. van den Bent MJ, Brandes AA, Taphoorn MJ, et al. Adjuvant procarbazine, lomustine, and vincristine chemotherapy in newly diagnosed anaplastic oligodendroglioma: Long-term follow-up of EORTC brain tumor group study 26951. J Clin Oncol 2013;31:344–50
72. Chamberlain MC, Born D. Prognostic significance of relative 1p/19q codeletion in oligodendroglial tumors. J Neurooncol 2015;125:249–51
73. Jiang H, Ren X, Zhang Z, et al. Polysomy of chromosomes 1 and 19: An underestimated prognostic factor in oligodendroglial tumors. J Neurooncol 2014;120:131–8
74. Zlatescu MC, TehraniYazdi A, Sasaki H, et al. Tumor location and growth pattern correlate with genetic signature in oligodendroglial neoplasms. Cancer Res 2001;61:6713–5
75. Dong S, Pang JC, Hu J, et al. Transcriptional inactivation of TP73 expression in oligodendroglial tumors. Int J Cancer 2002;98:370–5
76. Husemann K, Wolter M, Buschges R, et al. Identification of two distinct deleted regions on the short arm of chromosome 1 and rare mutation of the CDKN2C gene from 1p32 in oligodendroglial tumors. J Neuropathol Exp Neurol 1999;58:1041–50
77. Jia B, Choy E, Cote G, et al. Cyclin-dependent kinase 11 (CDK11) is crucial in the growth of liposarcoma cells. Cancer Lett 2014;342:104–12
78. Wazir U, Jiang WG, Sharma AK, et al. Guanine nucleotide binding protein beta 1: A novel transduction protein with a possible role in human breast cancer. Cancer Genomics Proteomics 2013;10:69–73
79. Apel A, Herr I, Schwarz H, et al. Blocked autophagy sensitizes resistant carcinoma cells to radiation therapy. Cancer Res 2008;68:1485–94
80. Hu YL, DeLay M, Jahangiri A, et al. Hypoxia-induced autophagy promotes tumor cell survival and adaptation to antiangiogenic treatment in glioblastoma. Cancer Res 2012;72:1773–83
81. Feletti A. The role of mitotic slippage, USP1-regulated apoptosis, and multiple treatments in the action of temozolomide in glioblastoma multiforme. Dipartimento di Scienze cardiologiche, toraciche e vascolari, Vol. Tesi di Dottorato (corsi e scuole). Padova Digital University Archive: Universita Degli Studi Di Padova 2013:46
82. Naumov VA, Generozov EV, Zaharjevskaya NB, et al. Genome-scale analysis of DNA methylation in colorectal cancer using infinium humanmethylation450 beadchips. Epigenetics 2013;8:921–34
83. Cheng Y, Geng H, Cheng SH, et al. KRAB zinc finger protein ZNF382 is a proapoptotic tumor suppressor that represses multiple oncogenes and is commonly silenced in multiple carcinomas. Cancer Res 2010;70: 6516–26
84. Cheng Y, Liang P, Geng H, et al. A novel 19q13 nucleolar zinc finger protein suppresses tumor cell growth through inhibiting ribosome biogenesis and inducing apoptosis but is frequently silenced in multiple carcinomas. Mol Cancer Res 2012;10:925–36